Available online at www.sciencedirect.com
SCIENCE DIRECT
Pergamon
Cement and Concrete Research 34 (2004) 2127–2134
CEMENT AND CONCRETE RESEARCH

Effect of loading rate on damage of concrete

Piti Sukontasukkul[a,*], Pichai Nimityongskul[b], Sidney Mindess[c]

[a]Department of Civil Engineering, King Mongkut's Institute of Technology-North Bangkok, Bangkok, Thailand
[b]School of Civil Engineering, Asian Institute of Technology, Pathumthani, Thailand
[c]Department of Civil Engineering, University of British Columbia, Vancouver, Canada

Received 20 August 2003; accepted 15 March 2004

Abstract

In this study, damage mechanics theory was used directly to determine the damage of concrete subjected to both static and impact compressive loadings. Two approaches based on the variations of (1) elastic modulus (E) and (2) strain rate ($\dot{\varepsilon}$), were used. Results from both approaches indicated that the damage to concrete at peak load depended mainly on the rate of loading, as it increased with increasing loading rate. The specimens subjected to impact loading were found to suffer higher damage than those subjected to static loading, as seen by the larger value of D at peak load (0.8–0.9 for concrete subjected to impact loading and 0.65 for concrete subjected to static loading). Beyond the peak, the strain energy was sufficient to cause the damage to increase to one ($D=1$) without any further applied load.

Keywords: Elastic moduli; Compressive strength; Damage mechanics

1. Introduction

The damage of concrete subjected to any type of loading can be measured in several ways. One approach is to use the theory of scalar continuum damage mechanics (SCDM). For a given set of test results, the damage can be determined directly using SCDM by measuring the variations in parameters, such as the elastic modulus (E), energy, microhardness, density, or strain rate.

In this study, the variations of two parameters: (1) E and (2) strain rate are introduced and used to determine the damage (D_i) of concrete subjected to static and impact loadings. Results are compared and discussed in terms of the differences on each approach and the effect of loading rate on the damage level.

2. Theory of damage mechanics [1,2]

Briefly, the deformation of materials under load depends on factors, such as atomic structure, composition, rate of loading, and temperature. To understand the deformation characteristics of each individual material completely, an extensive knowledge of its atomic and molecular structure is required. However, in practice, the general constitutive equations of the continuum model (load–deformation relationship) are obtained without considering the complexity of the atomic structure of using variables, such as stress, strain, and elastic modulus. Under applied loads, the material structure eventually begins to disintegrate and the load-carrying capacity is reduced. The state of deterioration of a material was characterized by Kachanov [1] using a dimensionless, scalar variable denoted as damage (D).

To define damage (D) [2], consider a damaged body (an apple) and a representative volume element (RVE) at a point M oriented in a plane defined by its normal $\vec{n}$ and its abscissa x along the direction $\vec{n}$ (Fig. 1). If δA represents the cross-sectional area of the RVE and δA_d represent the area of microvoids or microcracks that lie in δA, the value of damage, $D(M,\vec{n})$, is:

$$D(M,\vec{n}) = \frac{\delta A_d}{\delta A} \tag{1}$$

From the above expression, it is clear that the value of the scalar variable D is bounded by 0 and 1:

$$0 \le D \le 1 \tag{2}$$

* Corresponding author. Tel.: +66-2-913-2500; fax: +66-2-587-4337.
E-mail address: piti@kmitnb.ac.th (P. Sukontasukkul).

0008-8846/$ – see front matter © 2004 Elsevier Ltd. All rights reserved.
doi:10.1016/j.cemconres.2004.03.022

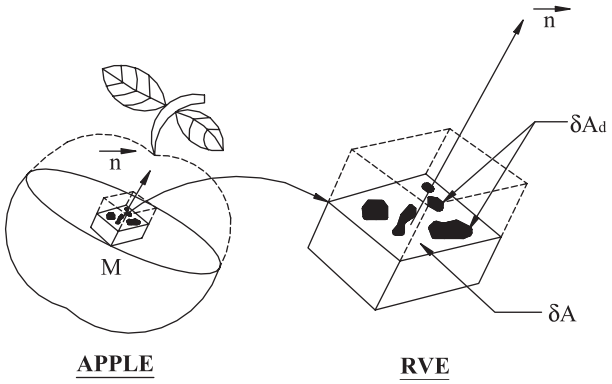

Fig. 1. A damaged body and RVE, after Lemaitre [2].

where $D=0$ corresponds to the intact or undamaged body; $D=1$ corresponds to the completely fractured body.

In the case of a simple two-dimensional homogeneous material, Eq. (1) is simplified to:

$$D = \frac{A_d}{A} \tag{3}$$

2.1. Variations of E approach

For any ductile material, the damage can be determined using the variations (degradation) of E as

$$D = 1 - \frac{E_{eff}}{E} \tag{4}$$

For a given load–deflection curve, Eq. (4) can be used to determine the damage of a loaded body.

However, in the case of a brittle material, such as concrete, a modification of Eq. (4) is necessary to make it more suitable. In ductile materials, E_{eff} is basically the change of E with respect to strain (or damage) after the loading goes beyond the linear stage and enters the plastic region (Fig. 2a). However, for a brittle material, such as plain concrete, the response is quite different; after reaching peak load, failure occurs abruptly (Fig. 2b). Therefore, to use CDM in concrete, the undamaged E is replaced by the initial E (E_{int}), while for the damaged E (E_{eff}), the secant E_{sec} is used instead. Eq. (4) is then rewritten as:

$$D_s = 1 - \frac{E_{sec}}{E_{int}} \tag{5}$$

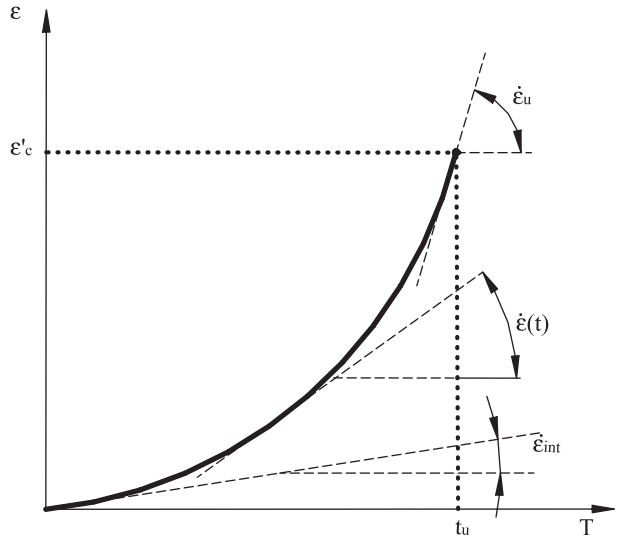

Fig. 3. Schematic illustration of the initial and the ultimate strain rate, and the strain rate at any time t.

2.2. Strain rate variation approach

In general, for a drop-weight impact test, the increase in strain up to the peak load is normally assumed to be linear (constant strain rate) to simplify the analysis. However, test results have indicated that the strain rate is, in fact, not constant. The strain rate was found to be slower at the beginning of the impact event, and then began to increase with the accumulation of damage [3].

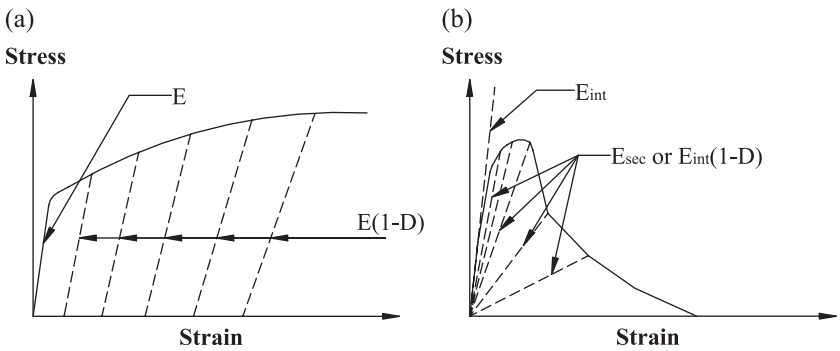

Fig. 2. Measurement of E for (a) ductile material and (b) brittle material.

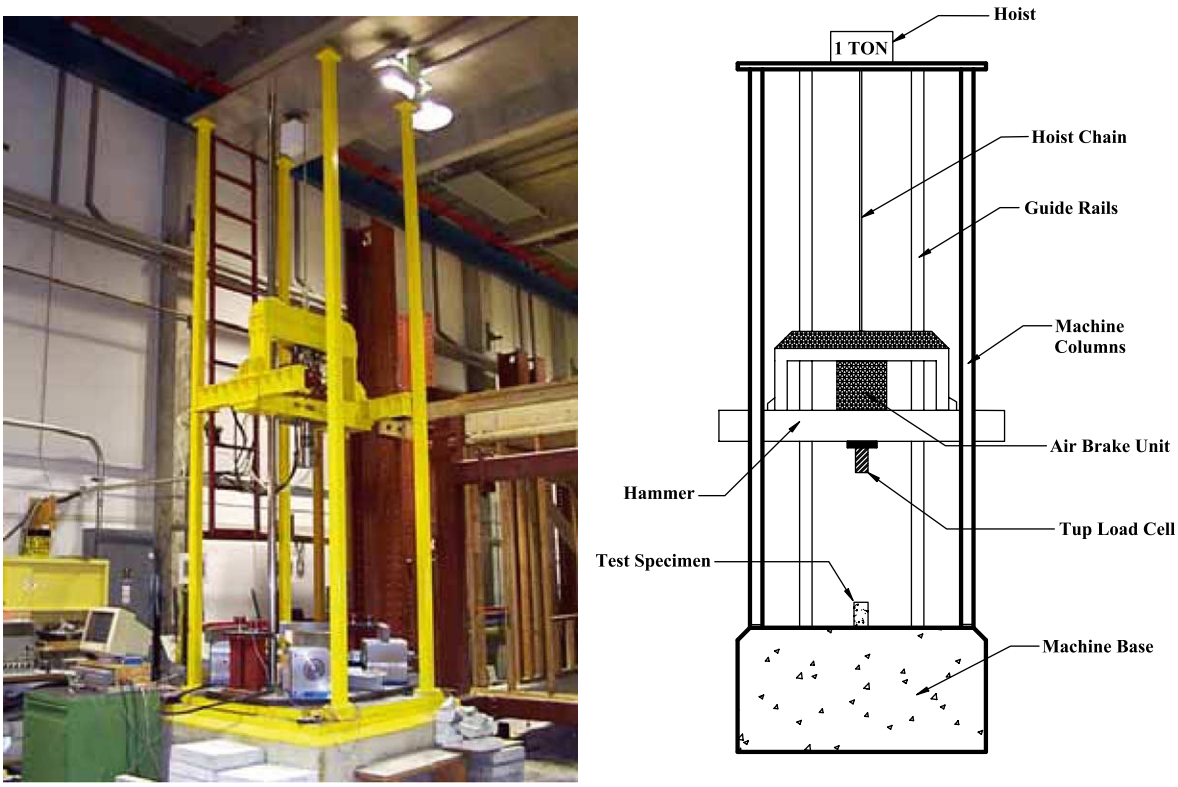

Fig. 4. Impact machine at UBC.

As a result, the damage of the material subjected to time-dependent loading can be expressed as (Fig. 3):

$$D_{\mathrm{i}} = 1 = \left(\frac{\dot{\varepsilon}_{\mathrm{int}}}{\dot{\varepsilon}(t)}\right)^{1/N} \tag{6}$$

where $\dot{\varepsilon}_{\mathrm{int}}$ is the minimum or initial strain rate (s^{-1}); $\dot{\varepsilon}(t)$ is the strain rate at any time t (s^{-1}); N is a temperature-dependent constant (assumed equal to 1).

3. Experimental program

The specimens with mix proportion of 1:0.5:2:2.5 (C/W/F/A) were cast using the following materials:

Cement: CSA Type 10 normal Portland cement (ASTM Type I)
Fine aggregates: clean river sand with a fineness modulus of about 2.7
Coarse aggregates: gravel with a 10-mm maximum size

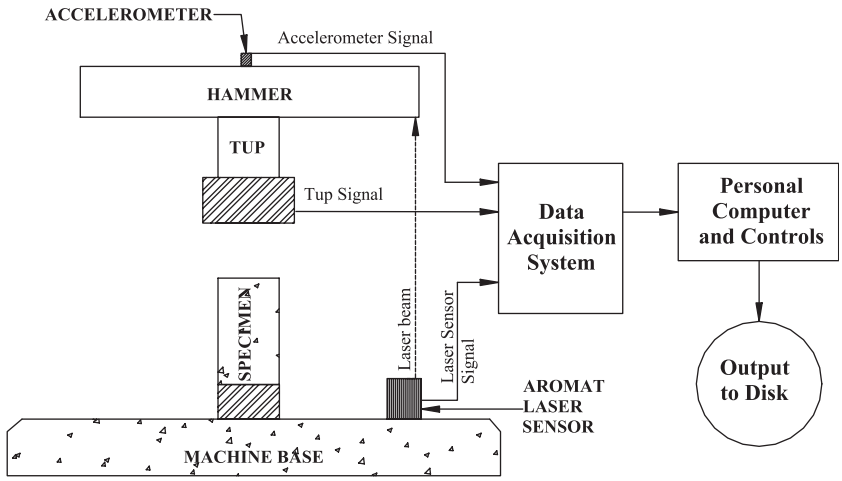

Fig. 5. Schematic illustration of the impact testing setup.

Table 1
Testing program

Designation	Description	Drop height (mm)	Number of specimen
Static test			
PLN	Concrete subjected to static loading	–	5
Impact test			
PL250	Concrete subjected to impact loading	250	5
PL500	Concrete subjected to impact loading	500	5

Concrete was prepared in the form of cylinders (diameter = 100 × 200 mm). Prior to mixing, the water content in the sand and aggregates was determined to adjust the amount of mixing water. The concrete was mixed using a pan-type mixer, placed in oiled steel molds in three layers; each layer was roughly compacted by rodding before being covered with polyethylene sheets. After 24 h, the specimens were demoulded and transferred to storage in a water tank for 30 days.

3.1. Static tests

All static tests were carried out at the Department of Civil Engineering, King Mongkut's Institute of Technology-North Bangkok (KMITNB) using a 1500-kN universal testing machine. Two Linear Variable Displacement Transducers (LVDTs) located on opposite sides of the specimen were used to measure the displacement. The rate of loading was controlled by the machine at 0.5 in./min. The data were collected by a PC-based data acquisition system.

3.2. Impact testing

All impact tests were carried out using an instrumented, drop-weight impact apparatus designed and constructed in the Department of Civil Engineering, University of British Columbia (UBC), and having the capacity of dropping a 578-kg mass from heights of up to 2500 mm on to the target specimen. The impact machine is shown in Fig. 4.

The specimen was placed vertically on a cylindrical steel base (diameter = 100 mm) located at the center of the impact machine, as shown in Figs. 4 and 5. The hammer was dropped from 250- and 500-mm heights to provide two different striking velocities of 2.21 and 3.13 m/s, respectively, and impact energies of 1417 and 2835 J, respectively. The testing program is summarized in Table 1.

In this test, two different indirect techniques were used (accelerometer and Aromat laser sensor) to measure acceleration and displacement, respectively. The accelerometer was placed on the impact hammer, while the Aromat laser sensor was placed on the impact machine base, about 500 mm away from the impact location for safety, with the laser aimed at the extension part of hammer. Because the accelerometer was attached to the hammer instead of the specimen, the recorded output was, in fact, the acceleration of the hammer. By assuming that the hammer displacement was essentially equal to the specimen deformation, the velocity and the displacement could be calculated using the equations below.

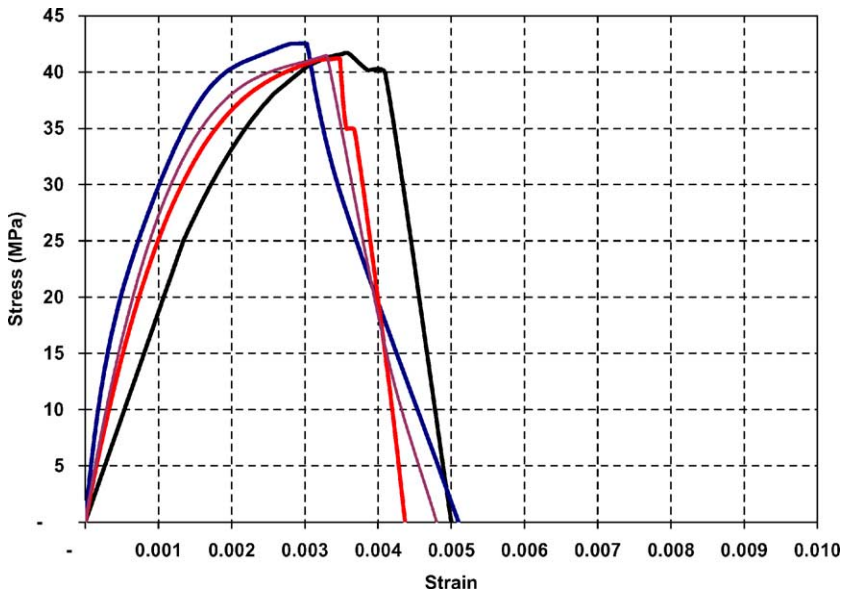

Fig. 6. Responses of concrete subjected to static loading.

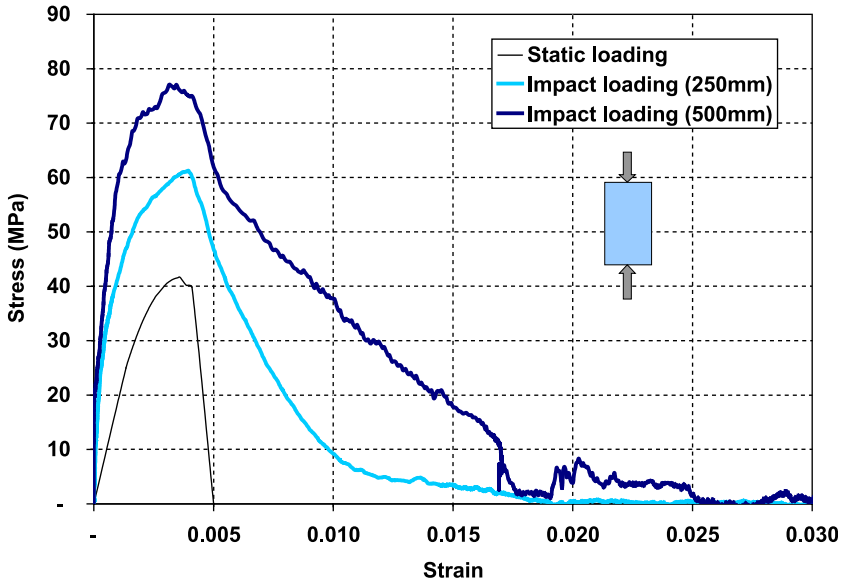

Fig. 7. Stress–strain curves of plain concrete subjected to static and impact loading.

From the initial potential energy, the hammer velocity, $\dot{u}_h(0)$, at beginning of the impact event is

$$\dot{u}_h(0) = \sqrt{2gh} \tag{7}$$

where g = corrected gravitational acceleration ($0.91 \times g$); h = hammer drop height.

At any time t after impact, the velocity $\dot{u}_h(t)$ is equal to

$$\dot{u}_h(t) = \dot{u}_h(0) + \int_0^t \ddot{u}_h(t)\mathrm{d}t \tag{8}$$

where $\ddot{u}_h(t)$ = recorded acceleration

Then, the displacement of the hammer, $u_h(t)$, at any time t becomes

$$u_h(t) = \int_0^t \left[\dot{u}_h(0) + \int_0^t \ddot{u}_h(t)\mathrm{d}t\right].\mathrm{d}t \tag{9}$$

For more details of Eqs. (7)–(9), please see Refs. [3,4].

For the Aromat laser sensor, the output was a displacement measurement and did not require any conversion. However, when the two displacements were compared, it was found that the displacements obtained from the Aromat laser sensor were higher than those obtained from the accelerometer, due to the cantilever deflection effect of the hammer extension arm during the impact event. Therefore, the displacements obtained by the Aromat laser sensor were considered to be an overestimate; they were instead used as an upper bound for checking those obtained by the accelerometer.

Table 2
Initial E of concrete

	Static (GPa)	Impact (GPa)	
		250 mm	500 mm
E_{int}	39	177	466

4. Results and discussion

4.1. Experimental results

4.1.1. Static loading

The typical stress–strain responses of concrete cylinders subjected to short-term static loading are shown in Fig. 6.

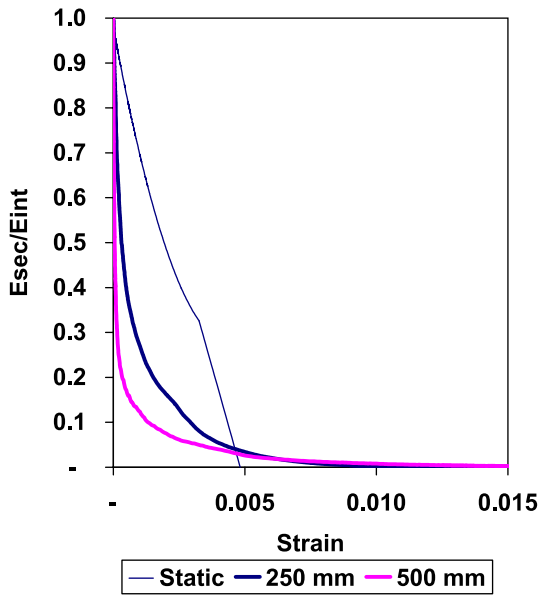

Fig. 8. Absolute E (E_{sec}/E_{int}) vs. strain.

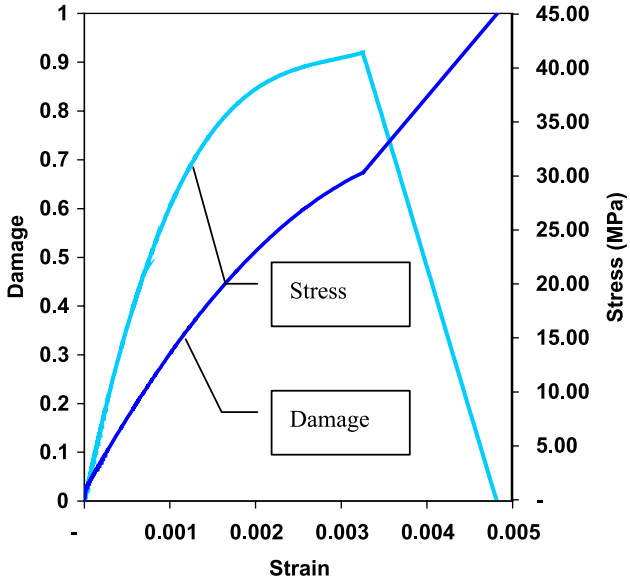

Fig. 9. Damage of concrete subjected to static loading.

It was found that the linear portion of the $\sigma-\varepsilon$ curve extended up to about 40–60% of peak load. Although a small amount of creep or other nonlinearity might occur in this linear portion, the deformation was essentially recoverable. At about 80–95% of the peak load, internal disruption began to occur, and small cracks appeared on the outer surface. These small cracks continued to propagate and interconnect until the specimen was completely fractured into several separate pieces. The formation and coalescence of the small cracks has long been recognized as the prime cause of fracture and failure of concrete, and of the marked nonlinearity of the stress–strain curve [5]. The deformation associated with cracks is completely irrecoverable, and may in some cases be considered as a quasi-plastic deformation. The load (or stress) at which the cracking becomes severe enough to cause a distinct nonlinearity in the $\sigma-\varepsilon$ curve is often referred to as the point of "discontinuity" [6]. At the peak load, the failure of concrete occurred in catastrophic manner, due to the large amount of energy that was released from the testing machine.

4.1.2. Impact loading

The concrete subjected to impact loading exhibited a quite different behavior from that subjected to static loading. The material behaved in a more brittle manner, and increases in strength, toughness, and modulus of elasticity were found as the rate of loading increased. Typical responses are given in Fig. 7.

For the specimens tested under impact loading, the linear portion of the $\sigma-\varepsilon$ curve extended to higher stress values than for specimens tested under static loading. This linear portion was also found to increase with increased rates of loading, as seen in the specimen tested at the highest rate of loading. Theoretically, the small cracks that cause the nonlinearity in the static case are forced to propagate much more quickly under impact loading. Thus, the cracks tend to propagate through rather than around aggregate particles, leading to an increase in strength and toughness, and a decrease in the nonlinear portion of the $\sigma-\varepsilon$ curve.

4.2. Damage of concrete

4.2.1. Variations of E approach

The E_{int} of concrete both under static and impact loading calculated from the test results are given in Table 2. Using these results, the absolute values of E (E_{int}/E_{sec}) were determined and plotted against the corresponding strains (Fig. 8).

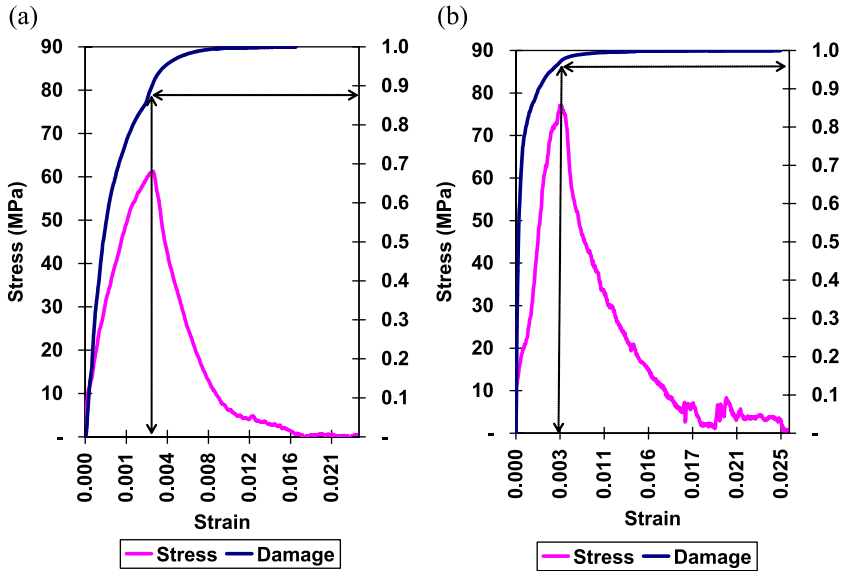

Fig. 10. Relationship between damage (E) and strain for concrete subjected to impact loading at (a) 250 mm and (b) 500 mm drop height.

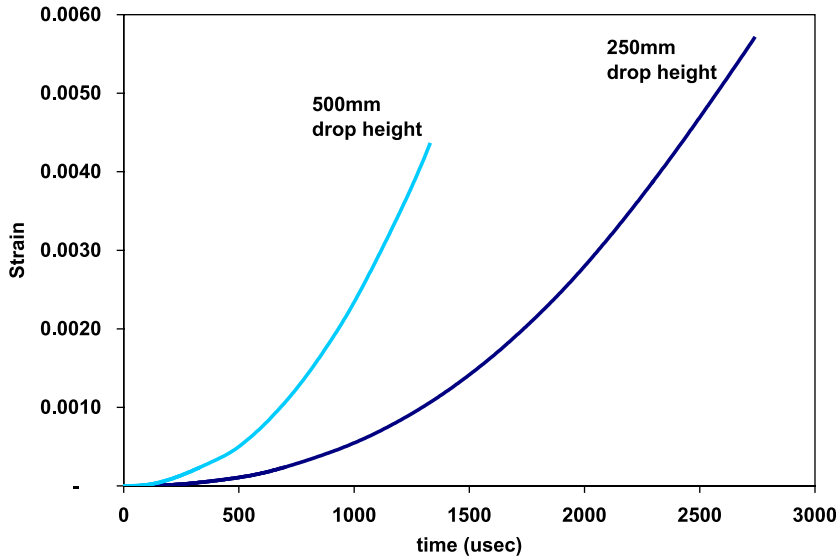

Fig. 11. Change of strain with time of concrete subjected to impact loading.

Results shown in Fig. 8 indicate that the degradation rate of E was faster with increasing loading rate. At the initial (undamaged) stage, the E_{sec} was essentially the same as E_{int}. However, with increasing load and deformation, the damage began to build up, and cracks started to form and propagate. The specimen continued to disintegrate and lose its stiffness. As a result, the value of E decreased at a dramatic rate.

Under impact loading, because cracks were forced to propagate at faster rate, the disintegration of the specimen was faster and so was the loss in stiffness, leading to the faster decay rate of E as seen in Fig. 8.

Once E_{int} and E_{sec} are already determined, the damage can simply be obtained using the procedure described earlier. Results are plotted in Figs. 9 and 10.

Under static loading, it may be seen that the damage of plain concrete can be represented by a nonlinear curve up to the peak and a linear curve after the peak (Fig. 9; it increases nonlinearly with strain from 0.0 up to 0.65 when it begins to slow down, and, right after the peak strain, it forms another straight line).

The damage at peak of plain concrete under static loading was found to be around 0.65. At the peak load, because of the material brittleness, the large amount of energy stored in the machine was released immediately, resulting in a sudden and catastrophic failure. This catastrophic failure also led to a rapid increase of damage of up to $D=1$ without a further increase in load.

Under impact loading, as for static loading, undamaged specimen exhibited a 0 value of D, and then with increasing

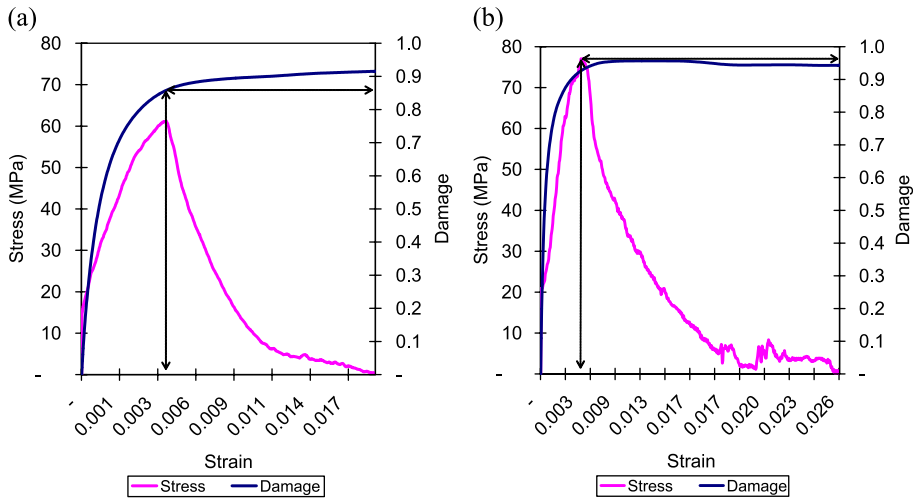

Fig. 12. Relationship between damage (strain rate) and strain for concrete subjected to impact loading at (a) 250 mm and (b) 500 mm drop height.

Table 3
Initial strain rate of concrete under impact loading

Strain rate	Impact (s^{-1})	
	250 mm	500 mm
$\dot{\varepsilon}_{int}$	0.00056	0.00151

stress (i.e., strain), the damage started to increase. Prior to the peak, the increasing rate of D was quite fast and almost proportional to the increase in stress and strain. The rate of increase slowed down after the peak load.

At the peak, the values of D increased nearly to 1 at both drop heights (0.872 and 0.961, respectively). The large value of D at the peak indicated that the specimen was, in fact, already in a state of high damage and almost completely fractured. After the peak, the strain energy was sufficient to cause crack propagation; hence, without any further application of load, the damage of the specimen kept on increasing to the value of 1.

The damage (value of D) was also found to be affected by the rate of loading (Figs. 9 and 10). The value of D at the peak for the specimens subjected to the higher impact velocity (3.13 m/s) was larger among than for those subjected to the lower impact velocity (2.21 m/s) and to static loading. This suggests that, with increasing rate of loading, the concrete is damaged more severely and pushed closer to a complete state of fracture.

4.2.2. Variations of strain rate

In addition to the variations of E, the variation of strain rate was also used to determine damage of concrete subjected to impact loading. Based on the test results, the change of strain with respect to time was plotted as shown in Fig. 11. As mentioned earlier, under impact loading, the strain rate actually changed with time. At the undamaged stage, the specimen was very stiff and strong, and thus, the rate of deformation (strain) was quite low. However, with further loading, the stiffness decreased gradually and the rate of deformation started to increase to a faster rate.

Once the strain rate corresponding to each strain is established, the damage can be determined using the procedure described earlier. Results are plotted in Fig. 12. The initial strain rates ($\dot{\varepsilon}_{int}$)of both impact tests are given in Table 3.

Prior to the peak, the values of D obtained by the strain rate variation approach (0.858 and 0.930) were quite similar to those obtained by the variations of E approach (0.855 and 0.952). Both were found to increase with stress in a similar manner, and up to the peak, the values of D approached 1. However, in this case, the value of D after peak never reached the value of 1 even at complete fracture. This was believed to be due to a limitation of Eq. (6) itself. For any given initial strain rate, the last term of Eq. (6) (the ratio between initial strain rate and strain rate at any time t) would not be equal to 0. Therefore, it is recommended here that this method is not a suitable measure of concrete damage.

Similar to the variations of E approach, the value of damage was also affected by the impact velocity. Increasing the drop height increased the level of damage in the specimens at every corresponding strain.

5. Conclusions

1. Damage mechanics can be used effectively to determine the damage of specimen subjected to static and impact loadings.
2. Both approaches (strain rate variation and degradation of E) exhibit similarity in determining damage prior to the peak load for concrete subjected to impact loading.
3. After the peak, the degradation of E approach is more realistic than the strain rate variation approach as seen by the convergence of D to the value of 1 at complete fracture.
4. It is found that the degradation of E and the level of damage of concrete at peak are both affected by the rate of loading. The degradation of E is faster and the level of damage at the peak load is found to be higher under impact loading. The level of damage, especially under impact loading, is very high (0.8–0.9) and closed to the level of fracture ($D = 1$).
5. After the peak, the strain energy is large enough to cause the damage to increase up to 1 (complete fracture) without having to apply any further load.

Acknowledgements

The authors would like to thank the Ministry of University Affairs and the Thailand Research Fund (TRF) for financially supporting this study.

References

[1] L.M. Kachanov, Introduction to Continuum Damage Mechanics, Kluwer Academic Publishing, Dordrecht, 1986.
[2] J. Lemaitre, A Course on Damage Mechanics, 2nd edition, Springer-Verlag, Berlin, 1996.
[3] P. Sukontasukkul, Impact Behaviour of Concrete under Multiaxial Loading, PhD thesis, University of British Columbia, Canada, 2001.
[4] N. Banthia, Impact Resistance of Concrete, PhD thesis, University of British Columbia, 1987.
[5] K. Newman, Criteria for the behavior of plain concrete under complex states of stress, Proceedings of an International Conference on Structure of Concrete: The Structure of Concrete and Its Behavior under Load, Cement and Concrete Association, London, UK, 1965, pp. 255–274.
[6] K. Newman, Concrete systems, in: L. Holliday (Ed.), Composite Materials, Elsevier, Amsterdam, 1966, pp. 336–452.